The Effect of Altered Lignin Composition on Mechanical Properties of CINNAMYL ALCOHOL DEHYDROGENASE (CAD) Deficient Poplars

Journal Article

Author(s):
Özparpucu, Merve; Gierlinger, Notburga; Burgert, Ingo; Van Acker, Rebecca; Vanholme, Ruben; Boerjan, Wout; Pilate, Gilles; Déjardin, Annabelle; Rüggeberg, Markus

Publication date:
2018-04

Permanent link:
https://doi.org/10.3929/ethz-b-000224839

Originally published in:
Planta 247(4), https://doi.org/10.1007/s00425-017-2828-z

Planta (2018) 247:887–897
https://doi.org/10.1007/s00425-017-2828-z

ORIGINAL ARTICLE

The effect of altered lignin composition on mechanical properties of CINNAMYL ALCOHOL DEHYDROGENASE (CAD) deficient poplars

Merve Özparpucu[1] · Notburga Gierlinger[3] · Ingo Burgert[1,2] · Rebecca Van Acker[4,5] · Ruben Vanholme[4,5] · Wout Boerjan[4,5] · Gilles Pilate[6] · Annabelle Déjardin[6] · Markus Rüggeberg[1,2]

Received: 15 September 2017 / Accepted: 8 December 2017 / Published online: 21 December 2017

Abstract

Main conclusion **CAD-deficient poplars enabled studying the influence of altered lignin composition on mechanical properties. Severe alterations in lignin composition did not influence the mechanical properties.**

Wood represents a hierarchical fiber-composite material with excellent mechanical properties. Despite its wide use and versatility, its mechanical behavior has not been entirely understood. It has especially been challenging to unravel the mechanical function of the cell wall matrix. Lignin engineering has been a useful tool to increase the knowledge on the mechanical function of lignin as it allows for modifications of lignin content and composition and the subsequent studying of the mechanical properties of these transgenics. Hereby, in most cases, both lignin composition and content are altered and the specific influence of lignin composition has hardly been revealed. Here, we have performed a comprehensive micromechanical, structural, and spectroscopic analysis on xylem strips of transgenic poplar plants, which are downregulated for cinnamyl alcohol dehydrogenase (*CAD*) by a hairpin-RNA-mediated silencing approach. All parameters were evaluated on the same samples. Raman microscopy revealed that the lignin of the *hpCAD* poplars was significantly enriched in aldehydes and reduced in the (relative) amount of G-units. FTIR spectra indicated pronounced changes in lignin composition, whereas lignin content was not significantly changed between WT and the *hpCAD* poplars. Microfibril angles were in the range of 18°–24° and were not significantly different between WT and transgenics. No significant changes were observed in mechanical properties, such as tensile stiffness, ultimate stress, and yield stress. The specific findings on *hpCAD* poplar allowed studying the specific influence of lignin composition on mechanics. It can be concluded that the changes in lignin composition in *hpCAD* poplars did not affect the micromechanical tensile properties.

Keywords Plant cell wall · Cell wall mechanics · Genetic modification · Lignin composition

Introduction

Wood is a hierarchically structured, multi-component fiber-reinforced composite. At the cell wall level, cellulose fibers are embedded in a matrix consisting of hemicelluloses and lignin (Cosgrove and Jarvis 2012; Mackenzie-Helnwein et al. 2005). The macroscopic mechanical behavior of wood is largely based on the complex organization of its cell walls (Speck and Burgert 2011). Although the role of cellulose microfibrils as load-bearing elements of the cell wall has been revealed, understanding the specific influence of the cell wall matrix on the mechanical behavior of the cell wall has proven to be more challenging.

In this respect, genetic engineering is a valuable tool to gain a better understanding of cell wall mechanics as it

Electronic supplementary material The online version of this article (https://doi.org/10.1007/s00425-017-2828-z) contains supplementary material, which is available to authorized users.

✉ Markus Rüggeberg
mrueggeberg@ethz.ch

1 Institute for Building Materials (IfB), ETH Zurich, 8093 Zurich, Switzerland

2 Laboratory of Applied Wood Materials, EMPA, 8600 Dübendorf, Switzerland

3 Institute for Biophysics, University of Natural Resources and Life Sciences Vienna, 1190 Vienna, Austria

4 Department of Plant Biotechnology and Bioinformatics, Ghent University, 9052 Ghent, Belgium

5 VIB Center for Plant Systems Biology, 9052 Ghent, Belgium

6 AGPF, INRA, 45075 Orléans, France

allows altering content, composition, and interconnection of the different cell wall polymers (Vanholme et al. 2008). Genetic engineering has been extensively utilized for creating plant lines with lower lignin content and/or altered lignin composition as both modifications may result in higher efficiency in pulping and bio-refinery processes (Baucher et al. 1996, 1998; Boerjan et al. 2003; Chen and Dixon 2007; Pilate et al. 2002; Van Acker et al. 2014; Vargas et al. 2016). In a number of studies, such transgenic plant lines have been studied by mechanical tests to reveal the mechanical function of lignin, both in terms of content and composition (Awad et al. 2012; Bjurhager et al. 2010; Hepworth and Vincent 1998; Horvath et al. 2010; Voelker et al. 2011). Horvath et al. (2010) analyzed the mechanical properties of *4-COUMARATE-CoA LIGASE (4CL)* downregulated poplars, which have a 30% reduction in Klason lignin content (Horvath et al. 2010). A decrease of specific bending stiffness (density normalized) of 40% was measured. In a recent study, Özparpucu et al. (2017) could correlate a reduction in tensile stiffness of 15% with a reduction of 12% in FTIR lignin absorbance (as an indication of lignin content) for young poplar trees downregulated for *CAD* via antisense (AS) and sense (S) gene silencing techniques (Özparpucu et al. 2017).

A few studies dealt with a mechanical analysis of transgenic plants with altered lignin composition but similar lignin content in comparison to the corresponding WT. Hepworth and Vincent (1998) found a 30% decrease in tensile elastic modulus of *CINNAMYL ALCOHOL DEHYDROGENASE (CAD)* downregulated tobacco plants with a similar Klason lignin content, but altered lignin composition. Yet, lignin content and composition were not analyzed on the samples investigated but taken from a previous study (Halpin et al. 1994), which had reported a lower S/G ratio for one transgenic line and the incorporation of cinnamaldehydes into lignin for both analyzed lines. A change in the S/G ratio may be mechanically relevant, as a syringyl-rich lignin has been considered as less condensed, due to less extended branching (Bonawitz and Chapple 2010). Horvath et al. (2010) performed three-point bending and compression tests on poplars produced by overexpression of *FERULATE 5-HYDROXYLASE* (*F5H*, named *PtrCAld5H* in the publication). An increase of the S/G ratio by a factor of two was observed. They found a non-significant decrease in bending elastic modulus of around 10% and a significant decrease in compression strength by 11%. Klason lignin content was lowered by 8% in comparison to the WT (Horvath et al. 2010).

In these studies, structural information, such as cellulose microfibril orientation, density, or lignin analysis, is either lacking or has not been taken from the mechanically tested samples. The importance of taking this information from the very same samples has been previously pointed out by Özparpucu et al. (2017). Furthermore, the importance of taking the structural organization of the cell wall into account for understanding the mechanical function of lignin has been revealed. The cellulose microfibril angles (MFA) of the plant fibers may play a crucial role in determining the specific influence of lignin (content and composition) on the mechanical behavior. At high angles, the cell wall matrix is loaded predominantly in shear, which may render lignin content and composition more relevant for the mechanical properties. The presence of lignin and its cross-linking to hemicellulose may increase shear stiffness and strength (Forbes and Watson 1992).

Using a hairpin-RNA-mediated silencing approach, *CAD*-downregulated poplar (*Populus tremula* × *P. alba*) lines, referred to as *hpCAD,* have been previously analyzed by van Acker et al. (2017). CAD catalyzes the last step in the biosynthesis of monolignols, namely the conversion from aldehydes to alcohols, and down-regulation of CAD expression results in the incorporation of mainly sinapaldehyde in the lignin polymer (Baucher et al. 1996; Lapierre et al. 1999; Van Acker et al. 2017). The *hpCAD* poplar lines displayed a homogeneous red colorization and had a very low residual CAD activity (~ 15% residual alcohol dehydrogenase activity). The study of Van Acker et al. revealed that Klason lignin content was reduced by approximately 8% and the composition of lignin was altered. Besides a significant incorporation of aldehydes into lignin, the syringyl (S)/guaiacyl (G) ratio was altered as compared to the corresponding WT. In the present study, we analyze *hpCAD* poplars for especially unravelling the influence of lignin composition on plant cell wall mechanics. The mechanical properties of xylem strips of *hpCAD* poplar were investigated by micromechanical tensile tests. To specifically reveal the influence of lignin composition on the mechanical properties, a comprehensive analysis of density, cellulose microfibril orientation, lignin content, and composition was conducted on the very same mechanically tested samples.

Materials and methods

Plant material

Three different *hpCAD* lines (*hpCAD4*, *hpCAD19*, and *hpCAD24*) were grown in the greenhouse with their corresponding WT for 3.5 months. At harvesting, the total stem length was on average 145 cm (without any significant difference between the three *hpCAD* lines and WT). For five biological replicates per line, the basal 10 cm stem segment was harvested, debarked, and immediately frozen until further usage for mechanical, structural and chemical analyses.

From the basal stem parts, sections of 30 mm length were taken to prepare tissue strips for mechanical, structural and

chemical (via spectroscopy) analyses. The outermost xylem was first removed by a microtome (Leica RM2255, Leica Microsystems, Germany), cutting to a depth of approximately 300 µm. Next, eight to fourteen consecutive longitudinal–tangential (LT) sections were cut from the stem with a thickness of 100 µm using a rotary microtome (Leica RM2255, Leica Microsystems, Germany). After microtome cutting, the width of the sections was trimmed to 1.5 mm using a scalpel. Cutting was done in wet conditions and the sections were kept in water until mechanical testing. The number of technical replicates tested for the five biological replicates of WT and the three *hpCAD* lines: *hpCAD4*, *hpCAD19*, and *hpCAD24* are given in Table 1.

Micromechanical tensile test

For the mechanical tests, a micro-tensile testing stage was used as described in Burgert et al. (2003). Displacement was recorded with video extensometry using a stereomicroscope and a CCD camera. The test length was fixed at 15 mm and a strain rate of 0.67‰ s^{-1} was used. Force was detected with a 50 N load cell (Honeywell, Sensotec Sensors). Based on the force–displacement curves, stress–strain curves were calculated. Then, elastic modulus, ultimate stress, yield strength, toughness, ultimate and yield strain values were evaluated. The bulk density of micromechanically tested samples was calculated with respect to green volume and oven-dry mass (Rowell 2012). For statistical analysis, first, the average value of the technical replicates was calculated for each of the five biological replicates per line and, next, the average of these five biological replicates was calculated for each line ($n = 5$, for *hpCAD4, hpCAD19*, and *hpCAD24*). Finally, the average values of the biological replicates were statistically compared using one-way ANOVA (Tukey's test range) at 95% ($p = 0.05$) confidence level.

Wide angle X-ray diffraction

Wide angle X-ray diffraction (WAXD) measurements were performed on the mechanically tested samples to analyze the cellulose microfibril orientation distribution and to calculate the microfibril angles (MFA) of the cell walls. For the measurements, a Nanostar (Bruker AXS, Germany) was used, equipped with a CuKα-source (wavelength of 1.54 Å) and operated in vacuum condition. On average, fifteen samples (from three biological replicates) were measured from WT

Table 1 Overview of the samples used to measure micromechanical tensile properties and MFA and to acquire FTIR and Raman spectra

Lines	Biological replicates	Number of technical replicates			
		Micromechanical tensile test	Microfibril angle (MFA) measurement[a]	FTIR measurement[b]	Raman mapping[c]
WT	WT-2	12	5	11	3
	WT-5	10	6	9	3
	WT-10	9	5	9	–
	WT-14	14	–	13	–
	WT-16	10	–	9	–
hpCAD4	*hpCAD4-11*	8	5	8	3
	hpCAD4-13	10	5	10	–
	hpCAD4-21	10	5	9	–
	hpCAD4-22	10	–	10	3
	hpCAD4-36	11	–	9	–
hpCAD19	*hpCAD19-10*	13	–	11	–
	hpCAD19-21	13	5	11	3
	hpCAD19-26	12	5	10	3
	hpCAD19-23	11	5	11	–
	hpCAD19-40	10	–	9	–
hpCAD24	*hpCAD24-2*	12	–	11	–
	hpCAD24-11	10	6	10	–
	hpCAD24-15	11	–	9	–
	hpCAD24-36	12	6	12	3
	hpCAD24-39	12	5	11	3

'–' no technical replicates analyzed

[a]Same technical replicates as used for the micromechanical tensile test

[b]Three spectra were acquired for each technical replicate and averaged

[c]Three mappings were done on one cross-section for each biological replicate

and each *hpCAD* line (Table 1). The X-ray beam diameter was set to approximately 300 µm and the sample-detector distance was set to 8.5 cm. One diffraction image was collected for each sample with an exposure time of 35 min. Azimuthal intensity profiles of the (200)-Bragg peak of crystalline cellulose were derived from the diffraction images by radial integration. The azimuthal profiles were used to calculate of the microfibril orientation distribution as explained in Rüggeberg et al. (2013).

Fourier transform infrared (FTIR) spectroscopy

FTIR measurements were conducted on the mechanically tested strips (LT cuts, for numbers, see Table 1). Measurements were done using an ATR (attenuated total reflection)-unit (Platinum, Bruker, Germany) on a TENSOR 27 FTIR spectrometer (Bruker, Germany). Three spectra were recorded on each strip (from left, middle and right parts) in the range of 4000–350 cm^{-1} with a spectral resolution of 4 cm^{-1}. The averaged spectra were used for further analysis. A total number of approximately 50 strips were investigated for each line. The averaged spectrum for each strip was baseline corrected and normalized to the strongest carbohydrate absorption band at 1034 cm^{-1}. The average spectra for each biological replicate were calculated and absorbance values (maximum height) of the bands in the fingerprint region (1800–800 cm^{-1}) were compared with statistical analysis using one-way ANOVA (Tukey's test range) at 95% ($p = 0.05$) confidence level.

Raman spectroscopy

Changes in the chemical composition of WT and *hpCAD* cell walls were elucidated in the sub-micrometer range using Raman microscopy. This spectroscopic technique allows for imaging the distribution and (relative) concentration of specific cell wall components. In addition, changes in lignin composition within the walls can be monitored (Gierlinger 2014). For the analysis, cross-sections with a thickness of 20 µm were cut using a rotary microtome from those parts of the stems that had been used for mechanical analysis. The sections were placed onto a glass slide with a drop of water and sealed with a coverslip and nail polish (Gierlinger et al. 2012). For each line, two biological replicates were chosen as specified in Table 1. Raman spectra were obtained in a confocal mode using a Raman spectrometer (InVia, Renishaw, UK) coupled to a microscope, and a linearly polarized green laser ($\lambda = 532$ nm) with a laser power of 19.6 mW. A 100 × oil immersion lens was used for high spatial resolution. Raman mappings were obtained utilizing line focus mapping with 0.3 µm step size, an integration time of 0.4 s per spectrum and a grating with a resolution of 1800 I/mm. Three mappings (at distances 300, 600, 1000 µm from cambium to pith) were conducted on each cross-section. For the evaluation of spectra, a cosmic ray removal (in Wire 3.7) was applied and the spectra were exported to Cytospec (Cytospec Inc., version 2.00.01) for further analysis. By integrating the intensity within the range of 1550–1650 cm^{-1}, which reflects the aromatic skeletal vibrations of lignin, Raman mappings showing the distribution of aromatic components within the cell walls were obtained. More detailed analysis was performed on the cell walls (CWL) and cell corners (CC) separately by defining three regions of interest (ROI) from CWL and CC on each mapping. The average spectra derived from each of these ROIs were treated by baseline correction and the normalization on the aromatic skeletal stretching vibration of lignin around 1600 cm^{-1} were analyzed in the software Opus 7.0.

Results

Micromechanical properties

The mechanical tests on thin xylem tissue strips of WT and *hpCAD* poplars revealed a stiffness and ultimate stress of approximately 2 GPa and 50 MPa, respectively (Fig. 1a, b and Table S1 in Supplementary material). No significant differences for these two parameters were detected between WT and the *hpCAD* lines. The stress–strain curves of WT and *hpCAD* showed a biphasic character (i.e., the curves have a clear yield point, Fig. S1a in Supplementary material). A yield stress of about 29 MPa was found for all lines, without any significant differences between WT and *hpCAD* lines (Fig. 1c). The wood density of the xylem strips appeared to be significantly lower for *hpCAD24* compared to WT, whereas no significant differences were found for the other two lines (Fig. 1d). Density directly affects the mechanical properties of wood tissue (Zobel and Van Buijtenen 2012); however, no significant differences were observed for the specific (density normalized) elastic modulus (Fig. S1b in Supplementary material).

Microfibril angle (MFA)

Wide angle X-ray diffraction was performed to determine the MFA on a subset of the xylem strips that were also used for the micromechanical tests. The X-ray analysis revealed average MFAs of 23° ± 3° for WT, 24° ± 2° for *hpCAD4*, 24° ± 5° for *hpCAD19* and 18° ± 2° for *hpCAD24*. No significant differences between WT and *hpCAD* lines were found via ANOVA statistical analysis (95% confidence level).

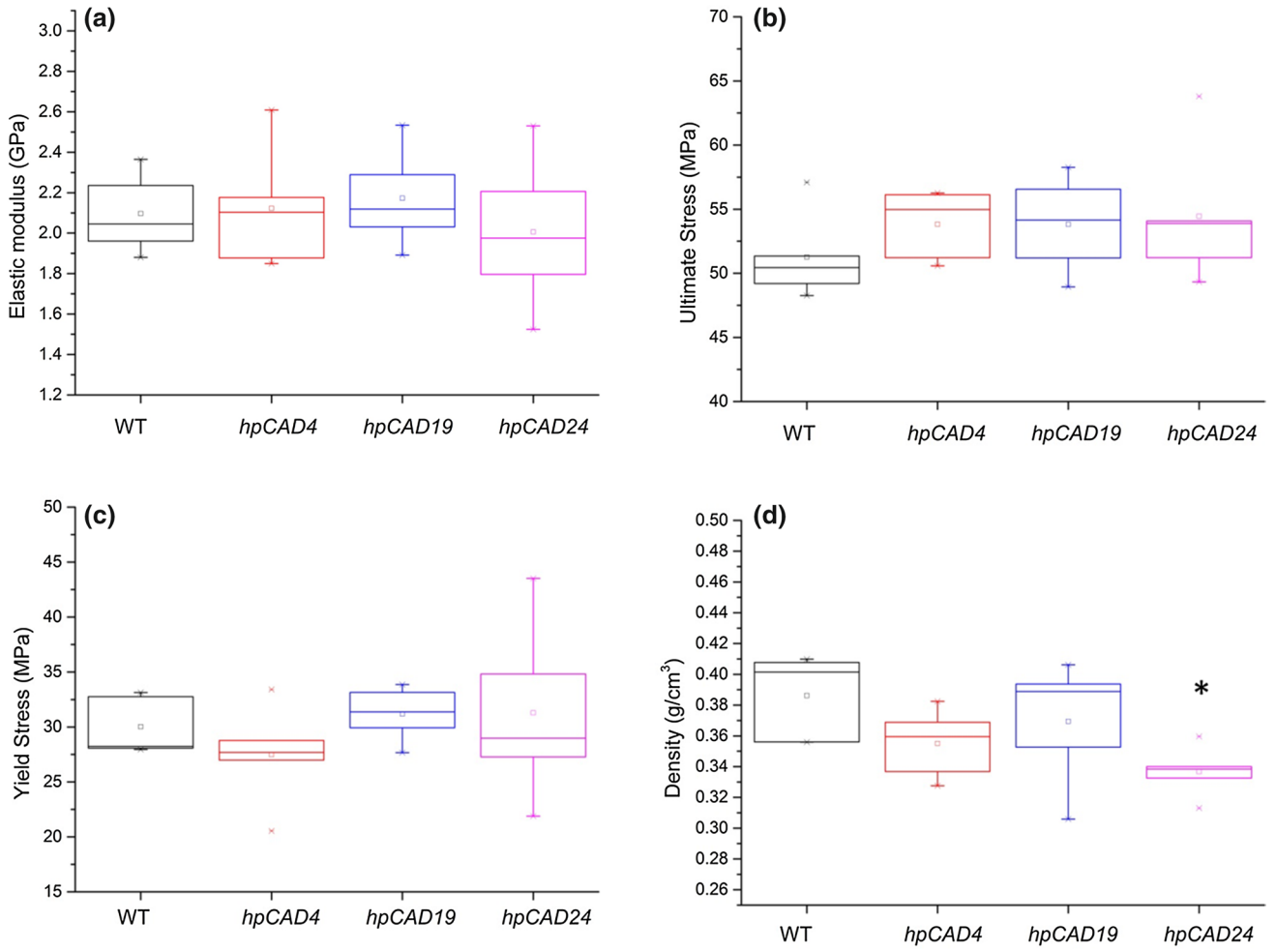

Fig. 1 Mechanical test results of WT and *hpCAD* lines. **a** Elastic modulus (GPa), **b** ultimate stress (MPa), **c** yield stress (MPa), and **d** wood density (g/cm^3), the lines inside the boxes denote the medians, the circle inside the boxes denote the average, the boxes mark the interval between the 25th and 75th percentiles, whereas the whiskers indicate the 1st and 99th percentile, outliers are shown as individual points (x). Asterisks indicate significant differences between WT and the transgenic lines at 95% confidence level (ANOVA test)

Lignin

FTIR

The average spectra of all three *hpCAD* lines (*hpCAD4, hpCAD19*, and *hpCAD24*) and WT are compared in the fingerprint region (1800–800 cm^{-1}) after baseline correction and normalization on the strongest cellulose band at 1034 cm^{-1} (Fig. 2). Since the spectra of the samples of the three *hpCAD* lines did not show any difference in terms of intensity values (absorbance) and the shape of the bands (see the second derivative FTIR spectra of each line in Fig. S2 in Supplementary material). Average spectra of the three *hpCAD* lines are shown in Fig. 2 and compared with the spectrum of WT. The intense carbohydrate bands in the range of 1187–860 cm^{-1} (C–O and C–C stretching) showed the same shape and position of maxima for all transgenic and WT plants, from which it can be concluded that cellulose structure was not affected by down-regulation of *CAD*. For the aromatic skeletal vibrations (plus C=O stretching) at 1593 and 1505 cm^{-1} (mainly lignin) (Faix 1991), a slight decrease of 3 and 6%, respectively, is visible in the spectra of *hpCAD* lines. However, these differences were found to be not significant at a level of $p = 0.05$ ($p_{1593} = 0.19$, $p_{1505} = 0.059$) for these bands (see Table S2 in Supplementary material).

Yet, a significantly lower absorbance was found in the spectra of *hpCAD* lines at 1460, 1424, and 1371 cm^{-1}. These bands can be assigned to C–H deformation (asymmetric in C–H3 and C–H2), aromatic skeletal vibrations combined with C–H deformations (in-plane), and aliphatic C–H bonds in methyl groups of lignin, respectively (Faix 1991). However, these bands may partly overlap with the bands originating from hemicellulose (at 1460 and 1423 cm^{-1})

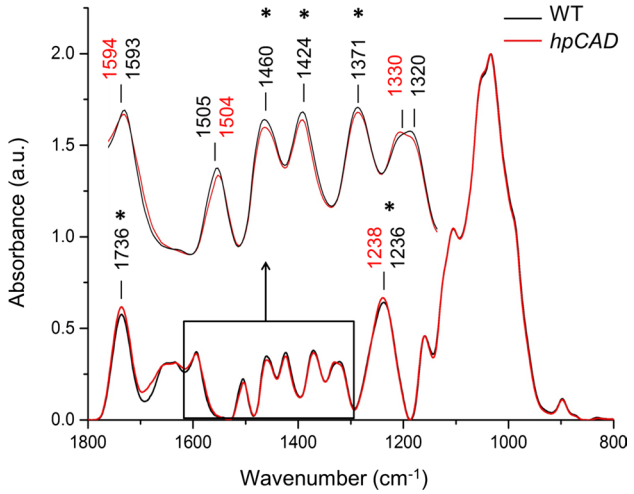

Fig. 2 Average FTIR spectra (normalized on the absorption at 1034 cm^{-1} and baseline corrected) of WT and *hpCAD* lines in the range of 1800–800 cm^{-1}. Asterisks mark absorption bands within the spectra which show significant differences in intensity between WT and the *hpCAD* lines according to ANOVA (Tukey's test) analysis at 95% confidence level. The total number of FTIR spectra for the calculation of average spectra is given in Table 1

and cellulose (at 1371 cm^{-1}) (Kačuráková et al. 1998). In addition, slight shifts in band positions were observed at 1593 cm^{-1} (aromatic skeletal plus C=O stretching, shifted to higher wavenumbers), 1505 cm^{-1} (aromatic skeletal, shifted to lower wavenumbers) and 1320 cm^{-1} (phenolic –OH deformations, shifted to higher wavenumbers) in *hpCAD* lines compared to WT, indicating changes in lignin composition of the transgenic lines.

Absorbance at 1736 and 1236 cm^{-1} was found to be significantly higher in the *hpCAD* lines. The band at 1736 cm^{-1} can be mainly assigned to C=O stretching of acetyl and carboxylic acid groups in xylan and to C=O stretching of unconjugated ketones in lignin. The minimum intensity next to the band at 1736 cm^{-1} (right) caused an additional shoulder at 1680 cm^{-1} in the second derivative spectra of the *hpCAD* lines compared to that of WT (Fig. 2 in Supplementary material). The band at 1236 cm^{-1} shows an intensity change and peak shift. It is assigned to asymmetric stretching of C–O–C in the acetyl groups of hemicellulose and pectin, but lignin also contributes to this band (Faix 1991; Schwanninger et al. 2004).

Raman

Raman images were generated by integrating the peak intensity of the bands characteristic for vibrations of aromatic plant cell wall components (1750–1550 cm^{-1}). Representative images are given in Fig. 3 for each of the *hpCAD* lines and WT, showing the intensity distribution of the aromatic ring stretching vibration at 1598 cm^{-1} (mainly aromatic stretching of lignin structures), C=C vibration at 1628 cm^{-1} (mainly from aromatic aldehyde structures, i.e., coniferaldehyde and sinapaldehyde structures), and C=C vibrations at 1656 cm^{-1} (mainly from coniferyl alcohol and sinapyl alcohol derived structures, but also C=O stretching of coniferaldehyde structures) (Agarwal 1999; Agarwal et al. 2011; Liu et al. 2015). The mappings of all aromatics reveal the well-known distribution of lignin in wood tissues with the highest concentration in the middle lamellae and the cell corners and with a lower concentration in the secondary cell walls (Fig. 3). WT and *hpCAD* lines do not show any (visible) difference in overall aromatic content (1598 cm^{-1}), but they show differences for the bands characteristic for aromatic aldehyde and coniferyl alcohol units. The band which is mainly attributed to aromatic aldehyde units (1628 cm^{-1}) shows high intensity in the *hpCAD* lines, whereas it is too small to be seen as a separate band between the two neighboring bands in WT. In contrast, the band mainly attributed to coniferyl and sinapyl alcohol units (at 1657 cm^{-1}) had a higher intensity in WT.

Furthermore, a region of interest (ROI) study was performed taking averaged Raman spectra from three cell corners and three cell walls of each mapping (for the numbers, see Table 1). Figure 4 shows the averaged spectra of the cell corners (CC) and cell walls (CWL) in the region of 1550–1700 cm^{-1} (baseline corrected and normalized at 1598 cm^{-1}).

The averaged spectra of the ROI study confirm the above described results of the mappings as the spectra of CC and the CWL of *hpCAD* plants show a clear band at 1628 cm^{-1}, which can be assigned to C=C vibration of sinapaldehyde and/or coniferaldehyde groups, while the band at 1657 cm^{-1}, which is characteristic of mainly coniferyl/sinapyl alcohol structures in the spectra of WT is hardly visible anymore in the spectra of *hpCAD* plants (C=C stretching of coniferyl alcohol and sinapyl alcohol) (Agarwal 1999; Liu et al. 2015). The Raman intensity at 1628 cm^{-1} in the spectra showed higher variability in the cell wall than in the cell corners, which points to a rather homogenous composition of the cell corner, but not of the cell walls. The aromatic stretching band at 1598 cm^{-1} shifted to slightly lower wavenumbers in the spectra of the transgenic lines for both cell corners and cell walls, which can be explained by changes in the substitution of the aromatic rings (Adapa et al. 2009; Sun et al. 2012).

Because the cellulose bands overlap with lignin bands in the region 1550–1100 cm^{-1}, the further study was restricted to the cell corner region (Fig. 3), as these represent almost pure lignin spectra. Differences between *hpCAD* lines and WT were found (normalized 1598 cm^{-1}, Fig. 5) and confirmed changes in lignin composition. Transgenic lines showed higher Raman intensity at 1503 cm^{-1} (asymmetric aromatic

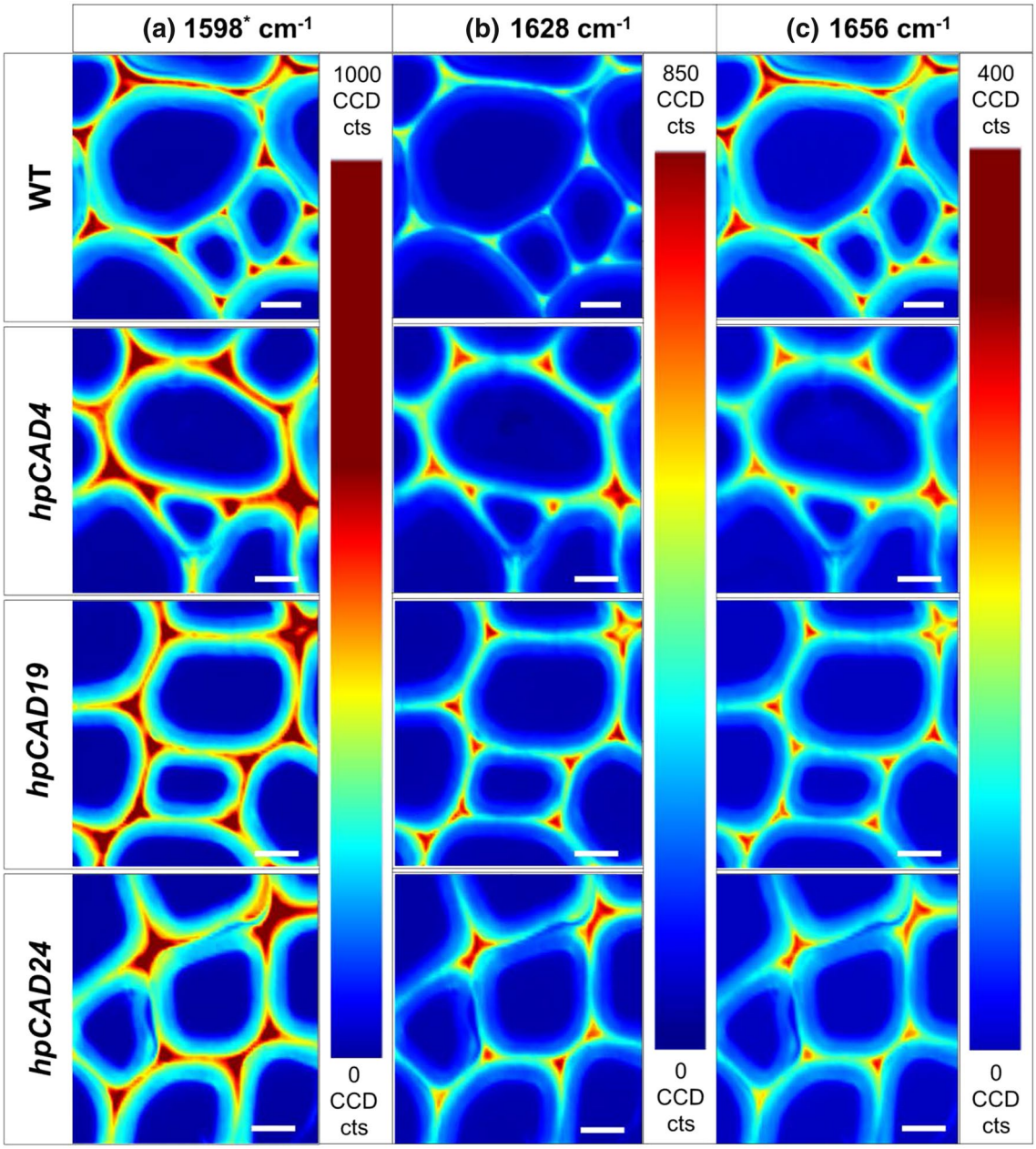

Fig. 3 Raman mapping images of WT, *hpCAD4*, *hpCAD19,* and *hpCAD24*, based on the integrated intensity of the band in the lignin aromatic region (1750–1550 cm^{-1}) at **a** 1598 cm^{-1} for WT, *1594 cm^{-1} for *hpCAD* lines (aromatic ring stretching of lignin), **b** 1628 cm^{-1} (C=C stretching of aromatic aldehydes) and **c** 1657 cm^{-1} (C=C stretching of coniferyl and sinapyl alcohol, plus C=O stretching of coniferaldehyde; Agarwal et al. 2011; Liu et al. 2015). Note the different intensity ranges of the color gradient for the different bands for better visibility of differences within each mapping; the scale bars indicate 10 µm

ring stretching of lignin), less intensity at 1460 cm^{-1} (assigned to CH_3 bending in the O–CH_3 group of lignin) and at 1269 cm^{-1} (assigned to aryl–O of aryl–OH and aryl-O–CH_3, which is known as a characteristic band of G-units (Agarwal et al. 2011) compared to the spectra of the WT plants. In addition, besides these intensity changes, some bands in the spectra showed shifts to higher wavenumber (e.g., 1377–1393 cm^{-1}: C–H bending in R3C–H, 1330–1333 cm^{-1}: aliphatic O–H bending and 1146–1162 cm^{-1}) compared to WT spectra.

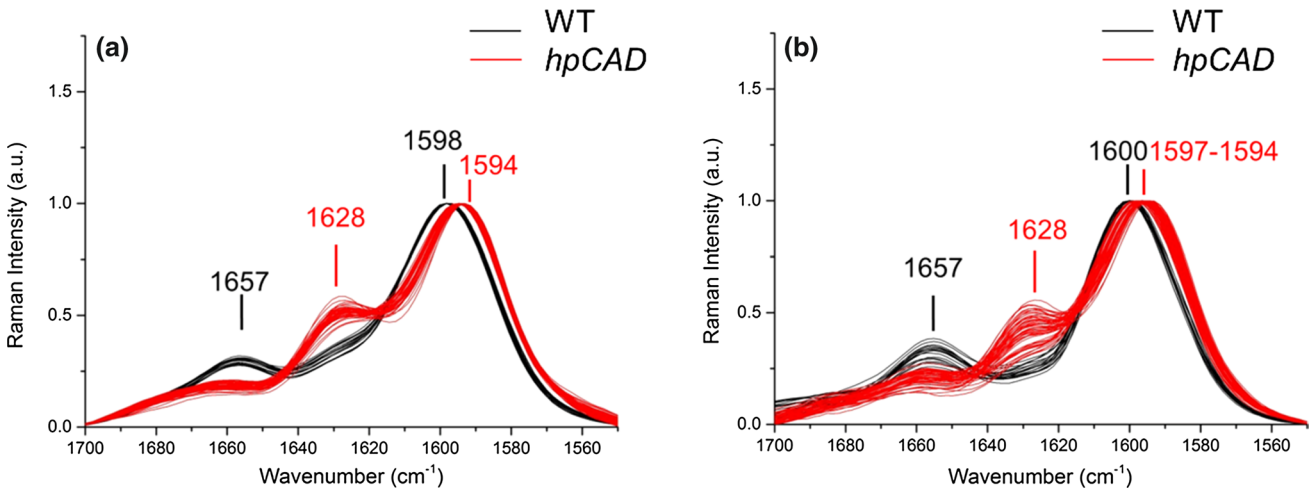

Fig. 4 Raman spectra of samples between 1700 and 1550 cm^{-1} (baseline corrected and normalized to the intensity at 1594–1600 cm^{-1}) of **a** cell corners (CC) and **b** cell walls (CWL). The bands at 1598 and 1594 cm^{-1} are attributed to aromatic ring stretching, the band at 1628 cm^{-1} to C=C vibration of mainly aromatic aldehydes, and the band at 1657 cm^{-1} mainly to C=C vibrations of mainly coniferyl and sinapyl alcohol derived structures and also to C=O stretching of coniferaldehyde structures (Agarwal et al. 2011)

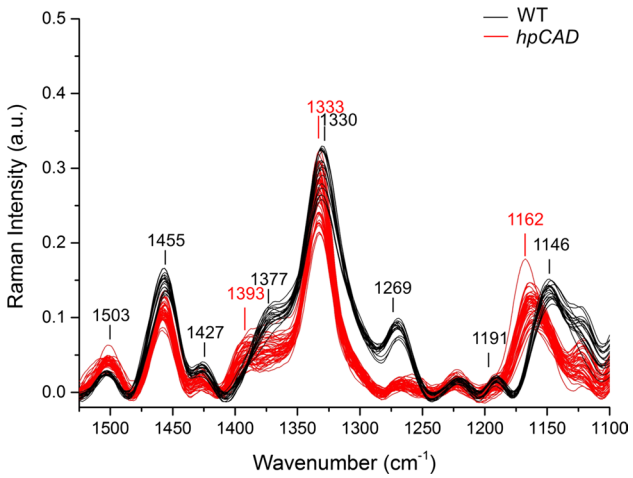

Fig. 5 Raman spectra of cell corners (CC) in the region between 1550 and 1100 cm^{-1} (baseline corrected and normalized on 1598 cm^{-1}), which confirm changes in lignin composition of *hpCAD* and WT lines

Discussion

Genetic engineering provides the possibility to specifically alter lignin content and/or composition, which provides the opportunity to reveal the role of lignin in plant cell wall mechanics. In the present study, we have mechanically, chemically, and structurally analyzed transgenic poplar plants with a reduced CAD activity, which was generated using a hairpin-RNA-mediated silencing approach (Van Acker et al. 2017). This has offered the possibility to specifically investigate the influence of changes in lignin composition on the mechanical behavior of poplar wood.

The changes in lignin composition have become evident in the Raman and FTIR spectra. In the Raman spectra, the occurrence of the 1628 cm^{-1} band (C=C stretching) gave proof of an increased aldehyde content in the transgenic lines. Aldehydes typically have a strong band around 1130 cm^{-1} reflecting the C–C stretching of the end group (C–C=O). As this band has a rather low intensity, an incorporation of aldehydes into lignin is suggested.

Previously, Van Acker et al. have performed wet chemistry analysis on the entire debarked stem of the same biological replicates of *hpCAD* poplar, which we have analyzed in the present study (Van Acker et al. 2017). By thioacidolysis followed by GC–MS and by NMR spectroscopy, an up to 20-fold increase in the incorporation of sinapaldehyde into lignin and a higher frequency of free-phenolic end-groups were measured, whereas no strong evidence was found for coniferaldehyde incorporation (Van Acker et al. 2017). Thus, our results on aldehyde incorporation are in-line with these findings, as in the Raman spectra, the band at 1630 cm^{-1} comprises the contribution of both types of aldehydes. The incorporation of sinapaldehyde may explain the changes in FTIR spectra visible for the range of 1800–1670 cm^{-1}. It is known that conjugated aldehydes and carboxylic acids show absorption bands at 1700 cm^{-1} and below. In addition, sinapaldehyde has a strong band at 1651 cm^{-1} (Faix 1991). The increased intensity at this wavenumber is considered to be responsible for the different shape of the shoulder around 1680 cm^{-1} (Fig. 2), which is even better visible in the second derivatives of the FTIR spectra (Fig. S2 in

Supplementary material). Additionally, it might also be the cause of the increased absorbance at 1736 cm^{-1} (Fig. 2).

The pronounced changes in the Raman spectra of *hpCAD* and WT in the region between 1550 and 1100 cm^{-1} mainly reflect a change in the ratio of the monolignol units. In particular, the transgenic lines showed a significant decrease in the band at 1269 cm^{-1}. Raman measurements on standard lignin compounds and on lignins derived from a number of plant species show that this peak is mainly assigned to guaiacyl (G) type of lignin (Agarwal et al. 2003, 2011; Larsen and Barsberg 2010; Sun et al. 2012). The band at 1330 cm^{-1} is shifted to 1333 cm^{-1} in *hpCAD* lines, but its intensity is not significantly different between *hpCAD* and WT lines. The band at 1330 cm^{-1} is often assigned to syringyl (S) type of lignin (Agarwal et al. 2003; Larsen and Barsberg 2010; Sun et al. 2012), but it can also comprise signals from G-units and is therefore not as specific as the G-unit band at 1269 cm^{-1}. The shift from 1146 to 1162 cm^{-1} may also reflect an increase of S-units as a similar shift is also observed between the spectra of poplar and spruce lignin, which differ in their S/G ratio (Gierlinger et al. 2013). When including the contributions of the aldehydes in the calculation of the S/G ratios of the lignins of WT and *hpCAD* poplars, the relative decrease of G-units is in line with the reported NMR results of the study of van Acker et al. (2017). The study reports an increase in S/G ratio of around 17% for the *hpCAD* poplars compared to WT. A higher incorporation of sinapaldehydes in *hpCAD* lines is also responsible for the higher intensity of the Raman band at 1503 cm^{-1}, which is assigned to aromatic ring stretching (Agarwal et al. 1997).

The changes in lignin composition of *hpCAD* lines are more pronounced compared to those of the AS/S-*CAD* lines (Özparpucu et al. 2017). The incorporation of aldehydes was much higher in *hpCAD* lines than in AS/S-*CAD* lines. In the Raman spectra, an intense band appeared at 1628 cm^{-1} in the spectra of the *hpCAD* lines, whereas only a shoulder at 1630 cm^{-1} was visible in spectra of AS/S-*CAD* lines (Özparpucu et al. 2017). In addition, the peak shifts detected in the FTIR spectra and the Raman spectra of *hpCAD* lines for several peaks were not visible for the spectra of the AS/S-*CAD* lines (Özparpucu et al. 2017).

While changes in lignin composition are much more pronounced in *hpCAD* lines compared to those measured in AS/S-*CAD* lines, the decrease in FTIR-lignin absorbance (at 1505 cm^{-1}, as an indicator of lignin content) was larger in AS/S-*CAD* lines. A significant decrease of 12% was found for AS/S-*CAD* lines, whereas a non-significant decrease of 6% was found in *hpCAD* lines in the current study. However, the severe changes in lignin composition may influence the intensity of the aromatic stretching vibration. Therefore, in the present study, changes in lignin content based on aromatic stretching vibrations detected by FTIR have to be taken with more care. The significantly lower absorbance present in the bands assigned to CH vibrations (e.g., 1460, 1424, and 1371 cm^{-1}) may rather be related to changes in lignin composition than to changes in lignin content.

For correlating changes in lignin composition with mechanical properties, density and cellulose microfibril orientation were analyzed, as they influence the mechanical properties of wood and may be affected as well (Bjurhager et al. 2010; Cave 1968; Donaldson 2008; Özparpucu et al. 2017; Salmén and Burgert 2009). No significant difference in MFA and wood density was found between WT and transgenic plants. Microfibril angles were measured in the range of 18°–24° for *hpCAD* lines and WT, which reflects typical values for juvenile wood (Gorisek et al. 1999). The values are very similar to those found for the AS/S-CAD plants (Özparpucu et al. 2017). For large MFA, it was shown that stiffness correlates with lignin content (Köhler and Spatz 2002; Özparpucu et al. 2017; Rüggeberg et al. 2008). The wood density appeared to be significantly reduced in one of the three lines tested (*hpCAD24*) only. Since MFA, wood density and lignin content were largely similar for WT and *hpCAD* plants and the micromechanical tensile tests did not reveal any significant differences in mechanical properties between WT and *hpCAD* lines, it can be concluded that the pronounced changes in lignin composition do not alter the tensile properties of the poplar wood to a measurable level.

These results are in line with the study of Horvath et al. (2010) on poplars overexpressing *F5H*, which reports a non-significant decrease in bending modulus of 9% for the transgenic lines, which exhibit an S/G ratio higher by a factor of two compared to the WT plant. This shift is much higher than that observed in *hpCAD*. This is also in line with the theoretical study of Jin et al. (2015), who simulated shear loading on a small representative volume element of the cell wall using molecular dynamics (MD) modeling. According to the simulations, a change in the S/G ratio by 20% (decrease as well as increase) does not lead to any changes in the shear stiffness of the matrix. Whereas these studies suggest that changes in lignin composition, i.e., changes in S/G ratio and incorporation of aldehydes, do not lead to changes in mechanical properties, it might be still possible that eventual changes in mechanical properties caused by the modification of lignin are masked by compensation mechanisms (Hu et al. 1999) or the rather pronounced variability in properties observed. Furthermore, other compositional changes of lignin may still have an influence on the mechanical properties.

Notably, WT and *hpCAD* lines of this study showed much higher variability in properties such as elastic modulus, lignin absorbance, and MFA, compared to WT and AS/S-*CAD* plants as reported in Özparpucu et al. (2017). The comparison of the coefficient of variance for these properties of both studies is given in Fig. S3 (Supplementary material). Moreover, the WT of *hpCAD* lines also showed higher

variability of all measured properties compared to WT of AS/S-*CAD* lines although they were grown in a common greenhouse environment (Özparpucu et al. 2017). Therefore, the high variability is likely of biological origin. It is worth to emphasize that studies revealing the structure–property relationships of young modified plants can be challenging in a way that resulting changes due to modification might be masked under natural variability. Thus, a comprehensive analysis with a high number of observations is crucial.

Conclusion

Significant changes in lignin composition were found for *hpCAD* poplars compared to WT plants. In particular, significant aldehyde incorporation into lignin and a relative decrease in G-units were observed. Lignin content was slightly, albeit not significantly, decreased. Neither microfibril orientation nor wood density was altered. A high microfibril angle in the range of 18°–24° was observed, which makes the mechanical properties of the cell wall matrix, in particular its shear stiffness, more relevant for the stiffness of the cell wall. Thus, changes in the composition of lignin, which alter the mechanical properties of the matrix, would be detectable by micromechanical analysis. The study revealed that micromechanical properties including stiffness, yield strength and ultimate strength of the transgenic plants were not significantly altered compared to WT plants. These settings offered the possibility of studying changes in lignin composition on cell wall and tissue mechanics without superimposed effects of changes in other structural features, which has rarely been possible so far. Thus, it can be concluded that the observed incorporation of cinnamaldehydes into lignin and the relative decrease in G-units, do not have a measurable influence on mechanical properties of poplar tissue and cell walls.

Author contribution statement MÖ conducted all lab experiments, evaluated the results, and wrote the manuscript. NG participated in performing spectroscopy studies and data evaluation. IB designed the study and participated in data evaluation of mechanics. RVA grew the plants. RV participated in data evaluation. WB participated in data evaluation. GP had developed the plant lines. AD had developed the plant lines. MR designed the study and participated in data evaluation and writing the manuscript. All authors participated in discussing the data and improving the manuscript.

Acknowledgements This work was supported by Grants from the Agency for Innovation by Science and Technology (IWT) through the SBO project BIOLEUM (Grant no. 130039) and the SBO-FISH project ARBOREF (Grant no. 140894), and the European Framework Project MultiBioPro (project number: 311804). R. V. is indebted to the Research Foundation Flanders for a postdoctoral fellowship. N. G. acknowledges funding by the Austrian Science Fund (START-project SURFINPLANT Y-728-316) and the European community (ERC-consolidator grant SCATAPNUT 681885).

Compliance with ethical standards

Conflict of interest The authors declare that they have no conflict of interest.

References

Adapa PK, Karunakaran C, Tabil LG, Schoenau GJ (2009) Potential applications of infrared and Raman spectromicroscopy for agricultural biomass. Agri Eng Int CIGR J XI:1081

Agarwal UP (1999) An overview of Raman spectroscopy as applied to lignocellulosic materials. In: Argyropoulos DS (ed) Advances in lignocellulosics characterization. Tappi Press, pp 201–225

Agarwal UP, Terashima N (2003) FT-Raman study of dehydrogenation polymer (DHP) lignins. In: Proceedings of 12th International Symposium Wood Pulping Chemistry, Department of Forest Ecology and Management, University of Wisconsin Madison, WI, pp 123–126

Agarwal UP, Ralph SA, Atalla RH (1997) FT Raman spectroscopic study of softwood lignin. In: Proceedings of 9th international symposium on wood and pulping chemistry (ISWPC), Montreal, pp 8-1

Agarwal UP, McSweeny JD, Ralph SA (2011) FT–Raman investigation of milled-wood lignins: softwood, hardwood, and chemically modified black spruce lignins. J Wood Chem Technol 31:324–344

Awad H, Herbette S, Brunel N, Tixier A, Pilate G, Cochard H, Badel E (2012) No trade-off between hydraulic and mechanical properties in several transgenic poplars modified for lignins metabolism. Environ Exp Bot 77:185–195

Baucher M, Chabbert B, Pilate G, Van Doorsselaere J, Tollier M-T, Petit-Conil M, Cornu D, Monties B, Van Montagu M, Inze D (1996) Red xylem and higher lignin extractability by down-regulating a cinnamyl alcohol dehydrogenase in poplar. Plant Physiol 112:1479–1490

Baucher M, Monties B, Montagu MV, Boerjan W (1998) Biosynthesis and genetic engineering of lignin. Crit Rev Plant Sci 17:125–197

Bjurhager I, Olsson A-M, Zhang B, Gerber L, Kumar M, Berglund LA, Burgert I, Br Sundberg, Salmén L (2010) Ultrastructure and mechanical properties of Populus wood with reduced lignin content caused by transgenic down-regulation of cinnamate 4-hydroxylase. Biomacromol 11:2359–2365

Boerjan W, Ralph J, Baucher M (2003) Lignin biosynthesis. Ann Rev Plant Biol 54:519–546

Bonawitz ND, Chapple C (2010) The genetics of lignin biosynthesis: connecting genotype to phenotype. Annu Rev Genet 44:337–363

Burgert I, Frühmann K, Keckes J, Fratzl P, Stanzl-Tschegg SE (2003) Microtensile testing of wood fibers combined with video extensometry for efficient strain detection. Holzforschung 57:661–664

Cave ID (1968) The anisotropic elasticity of the plant cell wall. Wood Sci Technol 2(4):268–278

Chen F, Dixon RA (2007) Lignin modification improves fermentable sugar yields for biofuel production. Nat Biotechnol 25:759–761

Cosgrove DC, Jarvis M (2012) Comparative structure and biomechanics of plant primary and secondary cell walls. Front Plant Sci 3:204

Donaldson L (2008) Microfibril angle: measurement, variation and relationships–A review. Iawa J 29:345

Faix O (1991) Classification of lignins from different botanical origins by FT-IR spectroscopy. Holzforschung-Int J Biol Chem Phys Technol Wood 45:21–28

Forbes JC, Watson D (1992) Plants in agriculture. Cambridge University Press, Cambridge

Gierlinger N (2014) Revealing changes in molecular composition of plant cell walls on the micron-level by Raman mapping and vertex component analysis (VCA). Front Plant Sci 5:306

Gierlinger N, Keplinger T, Harrington M (2012) Imaging of plant cell walls by confocal Raman microscopy. Nat Protoc 7:1694–1708

Gierlinger N, Keplinger T, Harrington M, Schwanninger M (2013) Raman imaging of lignocellulosic feedstock. In: Ven Tvd, Kadla J (eds) Cellulose–biomass conversion. INTECH, pp 159–192

Gorisek Z, Torelli N, Vilhar B, Grill D, Guttenberger H (1999) Microfibril angle in juvenile, adult and compression wood of spruce and silver fir. PHYTON-HORN 39:129–132

Halpin C, Knight ME, Foxon GA, Campbell MM, Boudet AM, Boon JJ, Chabbert B, Tollier MT, Schuch W (1994) Manipulation of lignin quality by downregulation of cinnamyl alcohol dehydrogenase. Plant J 6:339–350

Hepworth D, Vincent J (1998) The mechanical properties of xylem tissue from tobacco plants (Nicotiana tabacum 'Samsun'). Ann Bot 81:751–759

Horvath B, Peralta P, Peszlen I, Divos F, Kasal B, LaiGeng L (2010) Elastic modulus of transgenic aspen. Wood Res (Bratisl) 55:1–10

Hu W-J, Harding SA, Popko JL, Ralph J, Stokke DD, Tsai C-J, Chiang VL (1999) Repression of lignin biosynthesis promotes cellulose accumulation and growth in transgenic trees. Nat Biotechnol 17:808

Jin K, Qin Z, Buehler MJ (2015) Molecular deformation mechanisms of the wood cell wall material. J Mech Behav Biomed Mat 42:198–206

Kačuráková M, Belton PS, Wilson RH, Hirsch J, Ebringerová A (1998) Hydration properties of xylan-type structures: an FTIR study of xylooligosaccharides. J Sci Food Agric 77:38–44

Köhler L, Spatz H-C (2002) Micromechanics of plant tissues beyond the linear-elastic range. Planta 215:33–40. https://doi.org/10.1007/s00425-001-0718-9

Lapierre C, Pollet B, Petit-Conil M, Toval G, Romero J, Pilate G, Leplé J-C, Boerjan W, Ferret V, De Nadai V (1999) Structural alterations of lignins in transgenic poplars with depressed cinnamyl alcohol dehydrogenase or caffeic acid *O*-methyltransferase activity have an opposite impact on the efficiency of industrial kraft pulping. Plant Physiol 119:153–164

Larsen KL, Barsberg S (2010) Theoretical and Raman spectroscopic studies of phenolic lignin model monomers. J Phys Chem B 114:8009–8021

Liu B, Wang P, Kim JI, Zhang D, Xia Y, Chapple C, Cheng J-X (2015) Vibrational fingerprint mapping reveals spatial distribution of functional groups of lignin in plant cell wall. Anal Chem 87:9436–9442

Mackenzie-Helnwein P, Müllner HW, Eberhardsteiner J, Mang HA (2005) Analysis of layered wooden shells using an orthotropic elasto-plastic model for multi-axial loading of clear spruce wood. Comput Methods Appl Mech Eng 194:2661–2685. https://doi.org/10.1016/j.cma.2004.07.051

Özparpucu M, Rüggeberg M, Gierlinger N, Cesarino I, Vanholme R, Boerjan W, Burgert I (2017) Unravelling the impact of lignin on cell wall mechanics—a comprehensive study on young poplar trees downregulated for cinnamyl alcohol dehyrogenase (CAD). Plant J 91:480–490

Pilate G, Guiney E, Holt K, Petit-Conil M, Lapierre C, Leplé J-C, Pollet B, Mila I, Webster EA, Marstorp HG (2002) Field and pulping performances of transgenic trees with altered lignification. Nat Biotechnol 20:607–612

Rowell RM (2012) Handbook of wood chemistry and wood composites. CRC Press, Boca Raton

Rüggeberg M, Speck T, Paris O, Lapierre C, Pollet B, Koch G, Burgert I (2008) Stiffness gradients in vascular bundles of the palm Washingtonia robusta. Proceed R Soc B Biol Sci 275:2221–2229

Rüggeberg M, Saxe F, Metzger TH, Sundberg B, Fratzl P, Burgert I (2013) Enhanced cellulose orientation analysis in complex model plant tissues. J Struct Biol 183:419–428

Salmén L, Burgert I (2009) Cell wall features with regard to mechanical performance. A review COST Action E35 2004–2008: Wood machining–micromechanics and fracture. Holzforschung 63:121–129

Schwanninger M, Rodrigues J, Pereira H, Hinterstoisser B (2004) Effects of short-time vibratory ball milling on the shape of FT-IR spectra of wood and cellulose. Vib Spectrosc 36:23–40

Speck T, Burgert I (2011) Plant stems: functional design and mechanics. Annu Rev Mater Res 41:169–193

Sun L, Varanasi P, Yang F, Loqué D, Simmons BA, Singh S (2012) Rapid determination of syringyl: Guaiacyl ratios using FT-Raman spectroscopy. Biotechnol Bioeng 109:647–656

Van Acker R, Leplé J-C, Aerts D, Storme V, Goeminne G, Ivens B, Légée F, Lapierre C, Piens K, Van Montagu MC (2014) Improved saccharification and ethanol yield from field-grown transgenic poplar deficient in cinnamoyl-CoA reductase. Proc Natl Acad Sci 111:845–850

Van Acker R, Déjardin A, Desmet S, Vanholme R, Morreel K, Laurans F, Kim H, Santoro N, Foster C, Goeminne G, Légée F, Lapierre C, Pilate G, Ralph J, Boerjan W (2017) Different metabolic routes for coniferaldehyde and sinapaldehyde with CINNAMYL ALCOHOL DEHYDROGENASE1 deficiency. Plant Physiol 175(3):1018–1039. https://doi.org/10.1104/pp.17.00834

Vanholme R, Morreel K, Ralph J, Boerjan W (2008) Lignin engineering. Curr Opin Plant Biol 11:278–285. https://doi.org/10.1016/j.pbi.2008.03.005

Vargas L, Cesarino I, Vanholme R, Voorend W, Saleme MdLS, Morreel K, Boerjan W (2016) Improving total saccharification yield of Arabidopsis plants by vessel-specific complementation of caffeoyl shikimate esterase (cse) mutants. Biotechnol Biofuels 9:139

Voelker SL, Lachenbruch B, Meinzer FC, Strauss SH (2011) Reduced wood stiffness and strength, and altered stem form, in young antisense 4CL transgenic poplars with reduced lignin contents. New Phytol 189:1096–1109. https://doi.org/10.1111/j.1469-8137.2010.03572.x

Zobel BJ, Van Buijtenen JP (2012) Wood variation: its causes and control. Springer Science & Business Media, Berlin